International Forum on Aeroelasticity and Structural Dynamics
IFASD 2024
17-21 June 2024, The Hague, The Netherlands

GUST LOAD ALLEVIATION OF ELECTRIC AIRCRAFT WITH DISTRIBUTED PROPULSORS USING THRUST VECTORING

M. Amoozgar[1], G. Dimitriadis[2], J.E. Cooper[3], R. Ajaj[4]

[1]University of Nottingham
Nottingham, NG7 2RD, United Kingdom
m.amoozgar@nottingham.ac.uk

[2]University of Liège
4000 Liège, Belgium
gdimitriadis@uliege.be

[3]Bristol University
Bristol, BS8 1TR, United Kingdom
j.e.cooper@bristol.ac.uk

[4]Khalifa University of Science and Technology
P.O. Box 127788, Abu Dhabi, UAE
rafic.ajaj@ku.ac.ae

Keywords: Gust loads, electric aircraft, distributed electric propulsor, thrust vectoring, load alleviation

Abstract: In this paper, the effect of thrust vectoring of propulsors on gust load alleviation of an electric aircraft is investigated. The electric aircraft is composed of 6 small high-lift devices which are distributed equally along the wing span, and a cruise propulsor located at the tip of the wing. The aeroelastic behaviour of the wing is simulated by coupling the geometrically exact fully intrinsic beam equations with the Peters' unsteady aerodynamic model. A "1-cos" type gust is considered with various gust wavelength and speed. It is assumed that the propulsors are able to tilt their thrust vector in the pitch direction. The thrust of each propulsor is modelled using a follower force. Furthermore, it is assumed that the action point of propulsors' thrust has a chordwise offset from the wing elastic axis. First the developed numerical model is verified against the published results, and a very good agreement is observed. The results indicate that by pitching the thrust vector, it is possible to alleviate the gust loads. It is observed that the tip propulsor is more effective in gust load alleviation than the distributed high-lift propulsors. Furthermore, the results show that the thrust vectoring frequency is dependent on the gust wavelength. Finally, it is found that if the chordwise offset is zero, the torsional load can't be reduced by thrust vectoring, while by moving the propulsor ahead of the wing elastic axis, it is possible to alleviate all loads including torsional load.

1 INTRODUCTION

Due to environmental issue, the aviation industry has realised an urgent need for more environmentally friendly products such as electric aircraft. One of the potential solutions is to design a full electric aircraft with distributed electric propulsors (DEP) [1]. Since in this configuration several units of propulsors have been distributed along the wing span, it can bring several

benefits. One of the main benefits of a DEP configuration is its higher safety due to having higher number of propulsors [2]. Another key benefit is its lower noise emission due to the slower rotational speed of the rotor compared to fuel-based jet engines [3, 4]. There are a few more benefits such as better wing aerodynamic performance [2] and aeroelastic stability enhancement [5]. DEP configuration can possibly bring more potential benefits such as the one discussed in this paper. That's why in recent year, the design of aircraft with distributed propulsors has received a great attention.

The influence of distributed propulsors on lift to drag ratio of blended wing-body was considered by Leifsson et al [2]. Their findings indicate that the implementation of a Distributed Propulsion (DP) concept can lead to an improvement in the wing's lift-to-drag ratio. Patterson and German [6] investigated the impact of distributed propulsor positioning along the wing on its aerodynamic efficiency. The results showed that if the propulsors are placed at the wing leading edge, the wing lift can be enhanced more. Wing drag reduction due to distributing the propulsors along the span was studied by Stoll et al. [3]. The study utilized a leading-edge asynchronous propeller concept, demonstrating a 60% reduction in wing drag. Ma et al. [7] conducted a comparative study to examine the effect of a DEP concept on a vertical take-off and landing (VTOL) UAV. Their findings demonstrated that 34% of the aircraft's take-off weight is attributable to the propulsion system and cable weight, highlighting the challenges in designing a VTOL aircraft with a DP configuration. Erhard et al. [8] investigated aero-propulsive interactions in a Distributed Electric Propulsion aircraft using a low-fidelity method. Their study concluded that the overall aero-propulsive efficiency of the aircraft could be increased by up to 5.5%. Simmons and Murphy [9] investigated the wind tunnel-based model identification of a tilt-rotor wing with a Distributed Electric Propulsion configuration. The findings suggest that traditional aerodynamic modelling techniques must be adapted for application to these configurations. Burston et al [10] conducted a comprehensive review on the current efforts on the design and control of advanced DEP systems.

One of the main challenges of designing a wing with DEP configuration is that since the propulsors are distributed along the wing, the wing mass and stiffness are altered. This can directly impact the structural dynamics and subsequently the aeroelastic behaviour of the wing [10–13]. Not only this, but also the gust loads may also be altered due to the propulsors' mass, thrust and wake. It is already known that how the thrust can influence the wing aeroelastic stability [11, 14, 15], but its influence on gust loads has not been clarified. The position of the propulsor can affect the flutter speed of the wing, either increasing or decreasing it, particularly noticeable with highly flexible wings. Additionally, the aerodynamic interactions between the propellers and the wing could impact the aeroelastic characteristics of the wing. [16]. Aircraft structures must endure all the forces exerted on them during flight and ground maneuvers. Among the most severe dynamic loads encountered during flight are gust loads. While the aircraft may only face the most extreme gust conditions infrequently throughout its lifespan, its structure must still be designed to withstand these rare occurrences [17–19]. While it is desirable to design the wing structure in a way that it can withstand all such loads, an alternative way is to alleviate the gust loads. Castrichini et al. [20, 21] investigated the impact of employing a hinged wingtip to mitigate heavier load instances on the wing during flight. Their findings demonstrated that this mechanism has the potential to reduce the dynamic loads experienced by the wing. Szczyglowski et al. [17] examined the utilization of an inerter-based device for truss-braced wings to passively mitigate gust loads. Their findings indicated that employing a combination of inerter-based devices can result in a reduction of gust loads by 4%. Khalil and Fezans [22] devised a hybrid feedback/feedforward controller for a flexible aircraft's gust load alleviation system. The suggested approach relied on the H_∞-optimal control technique,

demonstrating its efficacy. More recently, Amoozgar et al. [19] showed the effectiveness of using a nonlinear energy sink to alleviate the wing gust loads. It was shown that the effectiveness of the NES in gust load alleviation is very sensitive to its design.
This paper proposes a new gust load alleviation concept for wings with distributed electric propulsors. It is assumed that the rotor disc can be tilted upward and downward sinusoidally to alter the thrust vector of the propulsor. An aeroelastic model is developed to evaluate the effectiveness of the proposed concept on gust load alleviation of a wing with DEP configuration.

2 PROBLEM STATEMENT

An electric aircraft wing similar to the NASA X-57 "Maxwell", as shown in Figure 1, is considered. The wing consists of one tip cruise propulsor and 6 high-lift motors which are distributed

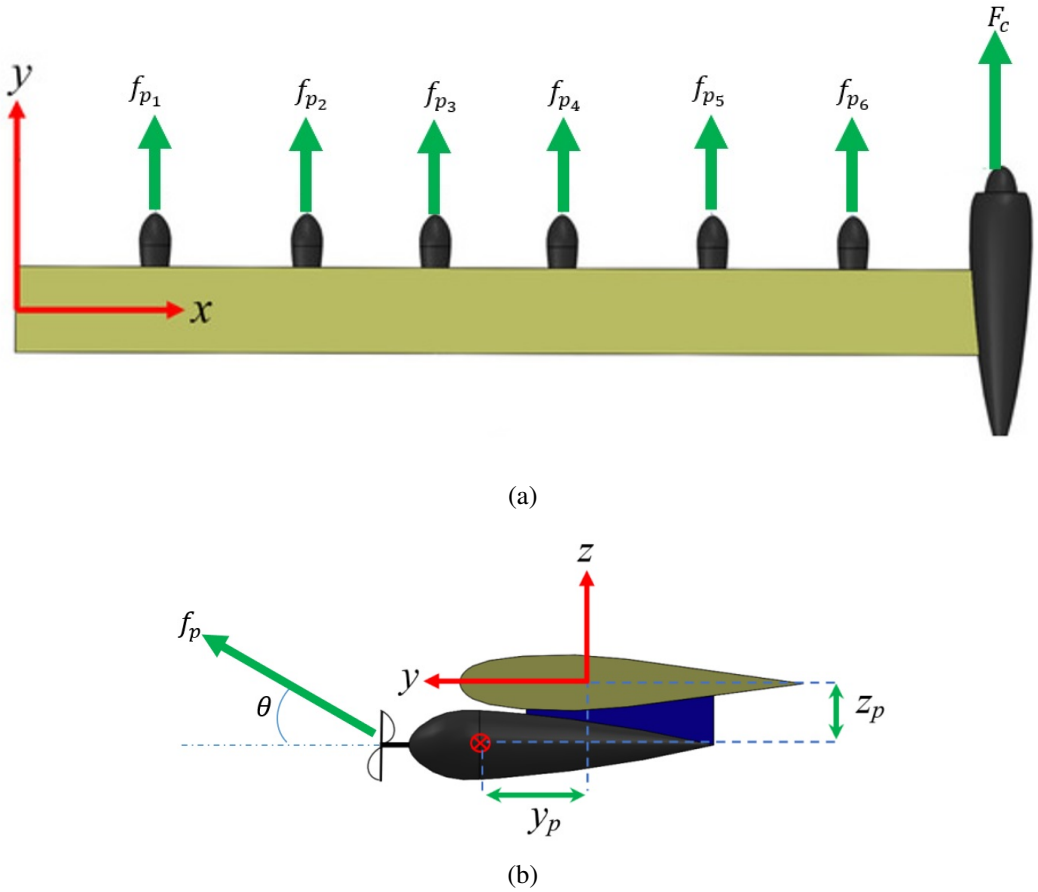

Figure 1: (a) A schematic of the wing with DEP configuration, (b) The wing/propulsor cross-section and thrust vectoring

equally along the wing span. All propulsors have a chordwise offset from the wing elastic axis denoted by y_p and thicknesswise of z_p. It is noted that in this study, there is no thicknesswise offset between the wing and propulsor (e.g. $z_p = 0$). It is assumed that the rotor disc of each propulsor can be tilted in the pitch directions with a maximum pitch angle denoted by θ. A follower force is applied to each propulsor to model the thrust. The follower force is directly acting on the centre of mass of propulsors. In what follows, the aeroelastic equations of this model are developed, and the effectiveness of thrust vectoring on gust load alleviation of the wing is investigated.

3 THE AEROELASTIC MODEL

The wing structural dynamics is modelled using the geometrically exact fully intrinsic beam formulation [23]. This model is then coupled with the 2D Peters' incompressible unsteady aerodynamic theory [23] to complete the wing aeroelastic equations as below

$$\boldsymbol{F'} + (\tilde{\boldsymbol{k}} + \tilde{\boldsymbol{\kappa}})\boldsymbol{F} - \dot{\boldsymbol{P}} - \tilde{\boldsymbol{\Omega}}\boldsymbol{P} + \boldsymbol{f_a} + \boldsymbol{f_T} = 0 \tag{1}$$

$$\boldsymbol{M'} + (\tilde{\boldsymbol{k}} + \tilde{\boldsymbol{\kappa}})\boldsymbol{M} + (\tilde{\boldsymbol{e_1}} + \tilde{\boldsymbol{\kappa}})\boldsymbol{F} - \dot{\boldsymbol{H}} - \tilde{\boldsymbol{\Omega}}\boldsymbol{H} - \tilde{\boldsymbol{V}}\boldsymbol{P} + \boldsymbol{m_a} = 0 \tag{2}$$

$$\boldsymbol{V'} + (\tilde{\boldsymbol{k}} + \tilde{\boldsymbol{\kappa}})\boldsymbol{V} + (\tilde{\boldsymbol{e_1}} + \tilde{\boldsymbol{\gamma}})\boldsymbol{\Omega} - \dot{\boldsymbol{\gamma}} = 0 \tag{3}$$

$$\boldsymbol{\Omega'} + (\tilde{\boldsymbol{k}} + \tilde{\boldsymbol{\kappa}})\boldsymbol{\Omega} - \dot{\boldsymbol{\kappa}} = 0 \tag{4}$$

where $\boldsymbol{F}$, $\boldsymbol{M}$, $\boldsymbol{V}$ and $\boldsymbol{\Omega}$ are internal force, moment, generalised linear velocity and angular velocity, respectively. $\boldsymbol{f_T}$ is the thrust force represented by the follower force, and $\boldsymbol{f_a}$ and $\boldsymbol{m_a}$ are the aerodynamic force and moment, respectively. Furthermore, $\boldsymbol{\gamma}$ and $\boldsymbol{\kappa}$ are the generalised strain and curvature measures which are related to the internal force and moment as follows

$$\begin{bmatrix} \boldsymbol{\gamma} \\ \boldsymbol{\kappa} \end{bmatrix} = \begin{bmatrix} \boldsymbol{R} & \boldsymbol{S} \\ \boldsymbol{S^T} & \boldsymbol{T} \end{bmatrix} \begin{bmatrix} \boldsymbol{F} \\ \boldsymbol{M} \end{bmatrix} \tag{5}$$

where $\boldsymbol{R}$, $\boldsymbol{S}$ and $\boldsymbol{T}$ are the beam cross-sectional flexibilities. Furthermore, the linear and angular velocities are related to the linear and angular momenta through the cross-sectional mass matrix such that

$$\begin{bmatrix} \boldsymbol{P} \\ \boldsymbol{H} \end{bmatrix} = \begin{bmatrix} \mu\boldsymbol{\Delta} & -\mu\tilde{\boldsymbol{\xi}} \\ \mu\tilde{\boldsymbol{\xi}} & \boldsymbol{I} \end{bmatrix} \begin{bmatrix} \boldsymbol{V} \\ \boldsymbol{\Omega} \end{bmatrix} \tag{6}$$

where μ is the mass per unit length of the beam, $\boldsymbol{I}$ is the mass moment of inertia matrix, $\boldsymbol{\xi}$ is the offset of the mass centre from beam reference axis, and $\boldsymbol{\Delta}$ is the identity matrix. Moreover, the aerodynamic force and moments are obtained on beam reference axis using the transformation matrix ($\boldsymbol{C_a}$)

$$\boldsymbol{f_a} = \boldsymbol{C_a}\boldsymbol{F_a} \tag{7}$$

$$\boldsymbol{m_a} = \boldsymbol{C_a}\boldsymbol{M_a} + \boldsymbol{C_a}\tilde{y_{ac}}\boldsymbol{F_a} \tag{8}$$

where $\boldsymbol{F_a}$ and $\boldsymbol{M_a}$ are the unsteady aerodynamic loads in the aerodynamic reference frame system which are obtained using the Peters' model [24] which for a symmetric airfoil ($C_{l0} = C_{d0} = C_{m0} = C_{ma} = 0$) can be written as [25, 26]

$$\begin{bmatrix} \boldsymbol{F_a} \end{bmatrix} = 2\pi\rho b \begin{bmatrix} 0 \\ (V_{a3} + \lambda_0)^2 \\ -\dot{V}_{a3}b/2 - V_{a2}(V_{a3} + \lambda_0 - \Omega_{a1}b/2) \end{bmatrix} \tag{9}$$

$$\begin{bmatrix} \boldsymbol{M_a} \end{bmatrix} = 4\pi\rho b^2 \begin{bmatrix} -V_{a2}\Omega_{a1}b/8 - b^2/32\dot{\Omega}_{a1} + b/8\dot{V}_{a3} \\ 0 \\ 0 \end{bmatrix} \tag{10}$$

where λ_0 is the inflow which can be determined using the equations

$$\lambda_0 = 1/2\boldsymbol{B}^T\lambda \tag{11}$$

$$\boldsymbol{A}\dot{\lambda} + \sqrt{V_{a2}^2 + V_{a3}^2}\lambda/b = (-\dot{V}_{a3} + b/2\dot{\Omega}_{a3})\boldsymbol{C} \tag{12}$$

where $\boldsymbol{A}$, $\boldsymbol{B}$ and $\boldsymbol{C}$ are constant vectors or matrices as defined in [24].
In this study, a "1-cos" gust disturbance is used which is defined as

$$\begin{aligned} w_g(t) &= \frac{w_{g_0}}{2}[1 - cos(\frac{2\pi V}{l_g}t)], \quad 0 \leq t \leq \frac{l_g}{V} \\ w_g &= 0, \qquad\qquad\qquad\qquad t \geq \frac{l_g}{V} \end{aligned} \tag{13}$$

where l_g, and w_{g_0} are the gust wavelength and the gust maximum velocity, respectively. The gust maximum velocity can be obtained as

$$w_{g_0} = w_{ref} \left(\frac{H}{106.14} \right)^{(1/6)} \tag{14}$$

$$\tag{15}$$

where H is the half gust wavelength, and w_{ref} is the reference gust velocity which is a function of the altitude as defined in regulations.
The combined aeroelastic equations are discretised using a central finite difference method, and interagted numerically. The effects of propulsors' thrust vectoring are simulated based on the method explained in [5].

4 RESULTS AND DISCUSSIONS

In the first step, to verify the developed aeroelastic model, the flutter speed of a wing with the properties presented in Table 1 is obtained and compared with those reported by Amoozgar et al. [27]. This comparison for a clean wing without the effect of propulsors is presented in Table 2. It is noted that for all the results from here on, a time-step of $dt = 0.005$ is used, since, as shown in Figure 2, this leads to a converged results.

Figure 3 shows the tip response of the clean wing (without propulsors) for three speeds which

Table 1: The considered wing properties

Parameter	Value
Wing semi-length	6.1 m
Chord length	1.83 m
Out of plane bending rigidity (EI)	9.77×10^6 N.m^2
Torsional rigidity (GJ)	0.99×10^6 N.m^2
Mass per unit length	35.7 kg/m
Wing moment of inertia per unit length	8.64 kg.m
Elastic axis offset from L.E.	33% chord
Centre of gravity offset from L.E.	43% chord
Aerodynamic centre offset from L.E.	25% chord
$dx_1, dx_2, ..., dx_6$	0.76 m
dx_t	1.52 m
Nominal cruise thrust	9814 N

are below, on and above the flutter speed, which clearly shows the onset instability speed. In this study, various gusts wavelength is considered. Figure 4 shows the change of gust velocity for gust wavelength from 18m to 214m and for reference gust velocity of $w_{ref} = 17.07$m/s.
Figure 5 shows the effect of four gust wavelengths on the flap, and twist responses of the wing tip at sea level and speed of $V = 100$m/s which is well below the flutter speed. The results show

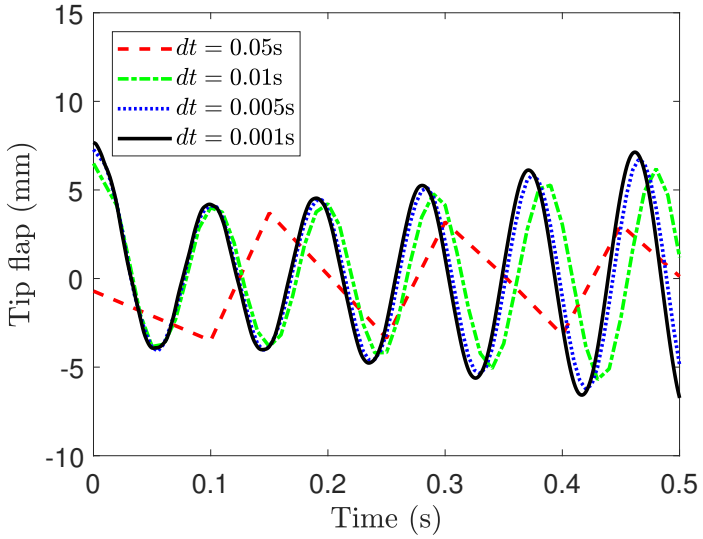

Figure 2: Time history of the wing tip for various time-steps and for $V = 145$ m/s

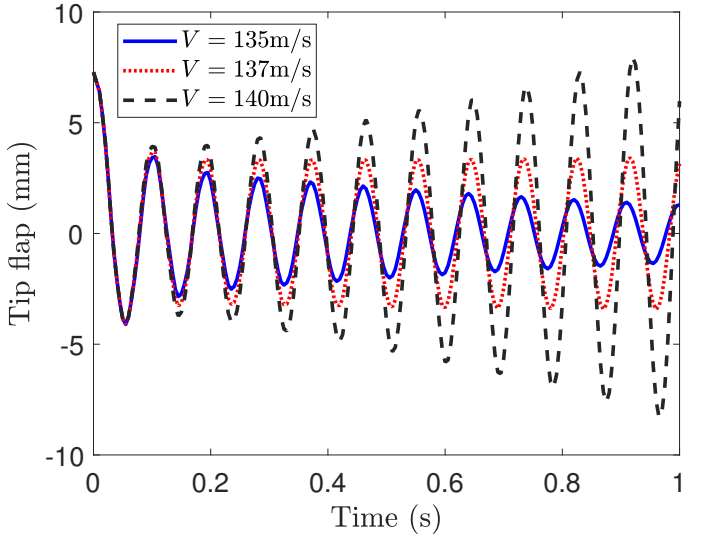

Figure 3: Time history of the clean wing tip response for various speeds

Table 2: Comparison of the flutter speed and frequency

Method	Flutter speed (m/s)	Flutter frequency (rad/s)
Present	136.8	69.9
Amoozgar et al. [27]	136	70

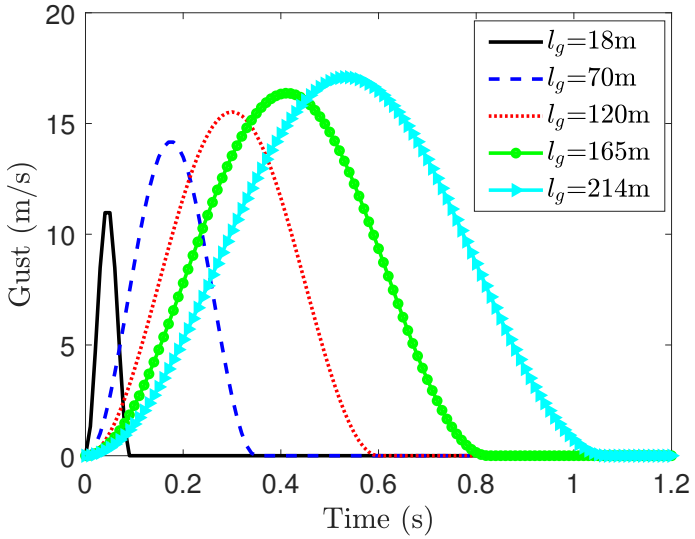

Figure 4: Gust velocity for different gust wavelength for $V = 200$ m/s and $w_{ref} = 17.07$ m/s

that the wing response is a function of the gust wavelength, and in this case, as the wavelength increases, the response peak also increases.

Next, the effect of gust wavelength and tip propulsor's thrust on the maximum and minimum values of quantities of interest (QI) (e.g. shear force, bending moment and torsion) for wing root at sea level are determined and shown in Figure 6. It is noted that here, the thrust is nondimensionalised with the nominal cruise thrust value specified in Table 1. The results shows that the shear force and bending moment do not change much by adding the thrust of propulsors, while the torsional load is affected to some extent. Also, the maximum and minimum loads are dependent on the gust wavelength. Figure 7 shows the same analysis for the effect of high-lift motors' thrust. Comparing this with the tip propulsor's thrust (6), it is clear that the gust alods are not affected too much with the level of thrust of high-lift propulsors, and hence from here onward, the focus of this study will only be on the effect of tip propulsors on wing gust loads.

The effect of reference gust velocity on the QIs are determined next and presented in Figure 8 for various values of tip propulsor's thrust. As the gust reference velocity increases, all load levels change, and the change is uniform. Hence, in all the upcoming studies, only one reference gust velocity is considered since the conclusion will stay the same irrespective of how much is the gust reference velocity. Here again it is the torsional loads that is being affected the most by increasing the thrust level.

Now, it is assumed that the tip propulsor thrust is able to be tilted in the pitch direction sinusoidally as described below

$$\Theta(t) = \theta sin(\omega_v t) \tag{16}$$

where θ is the maximum pitch angle, and ω_v is the pitching frequency.

Figure 9 shows the effect of thrust vectoring on gust response of the wing for the QIs at nominal cruise thrust for various maximum pitch angles. When the thrust vector tilts, it will make

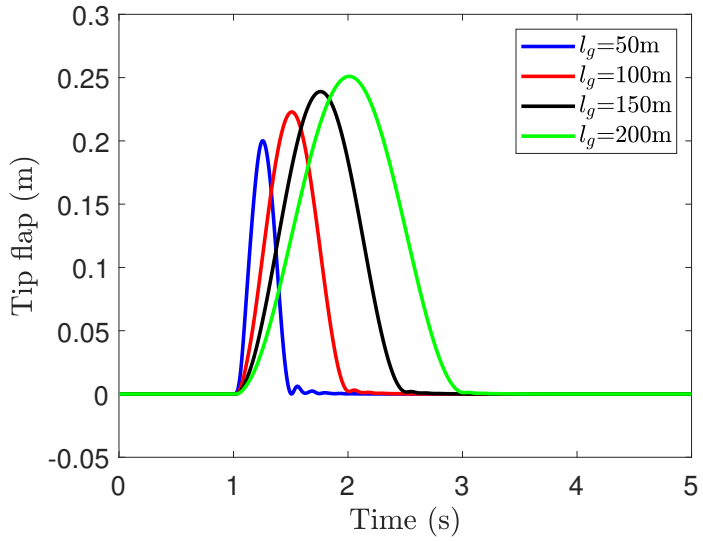

(a)

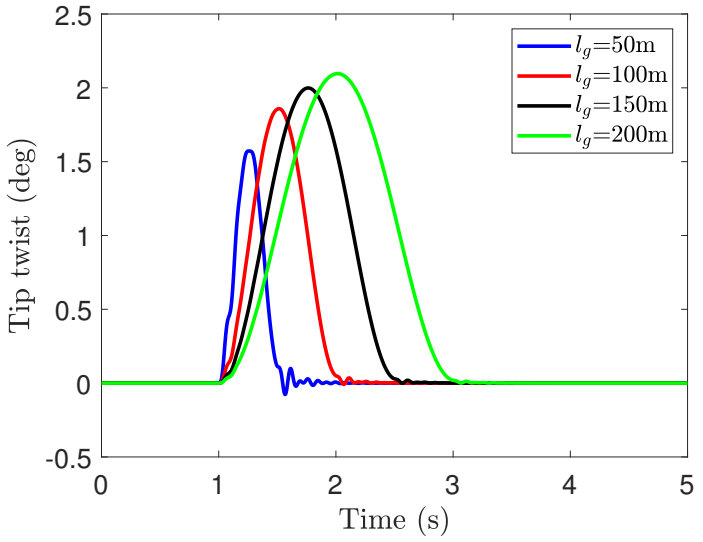

(b)

Figure 5: The effect of gust wavelength of (a) flap and (b) twist response of the wing tip for $V = 100$ m/s and $w_{ref} = 17.07$ m/s

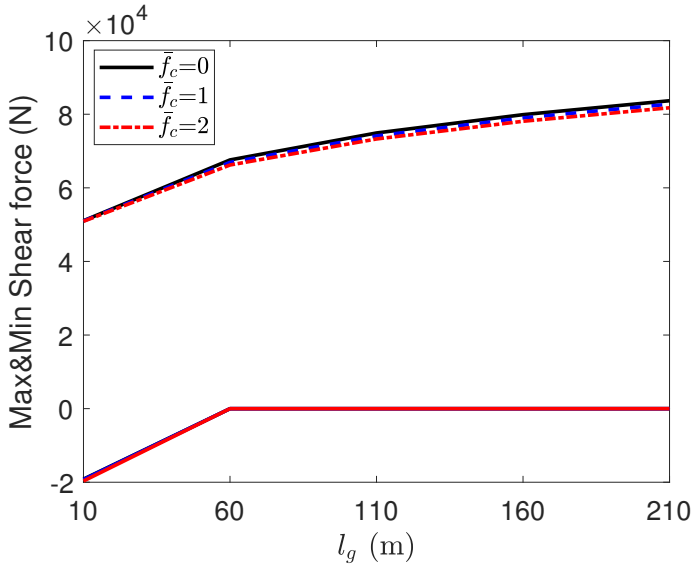

(a)

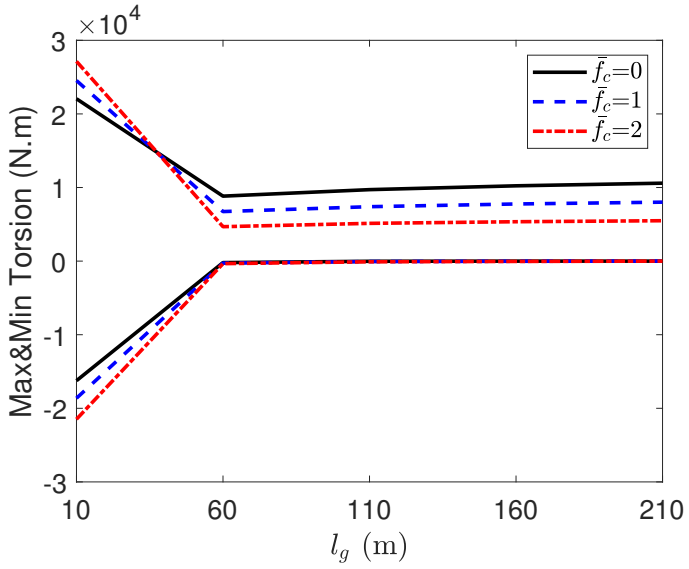

(b)

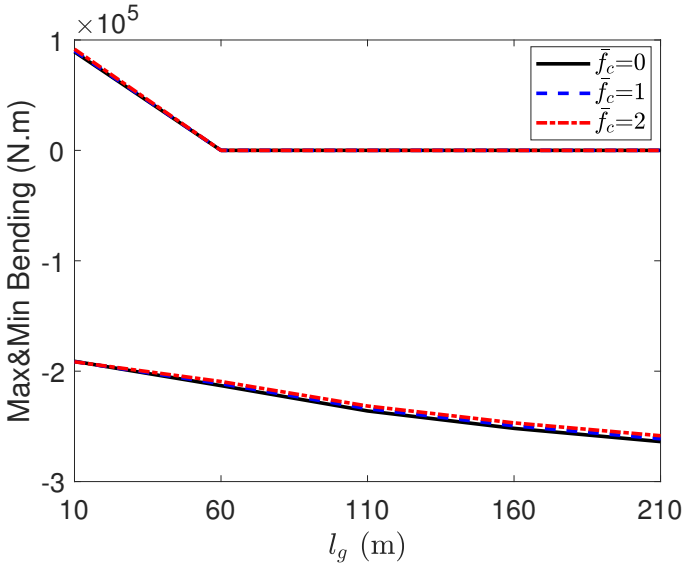

(c)

Figure 6: The effect of gust wavelength and tip propulsor on (a) shear force, (b) torsional and c) bending moment of the wing root for $V = 100$ m/s and $w_{ref} = 17.07$ m/s

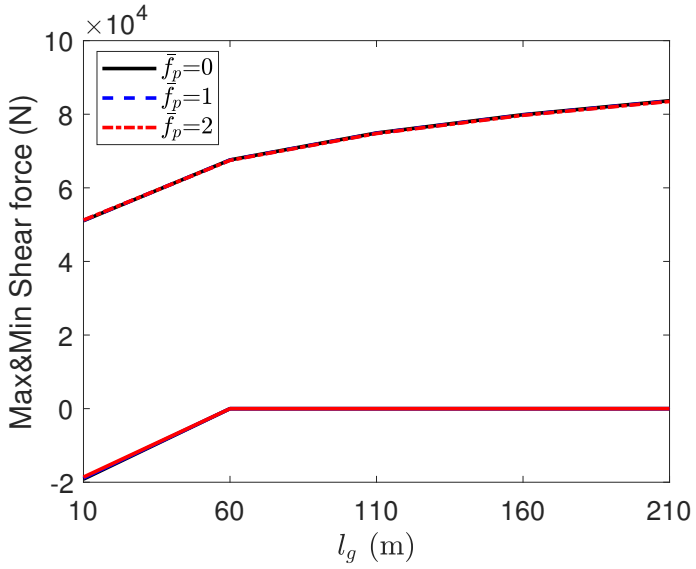

(a)

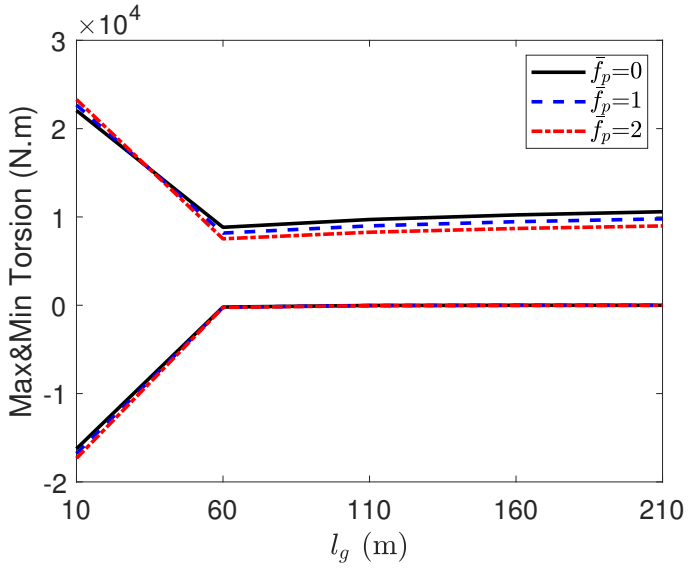

(b)

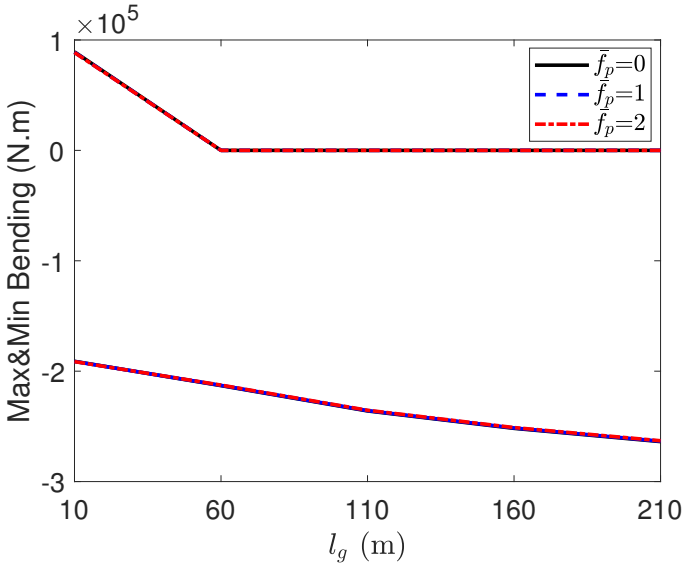

(c)

Figure 7: The effect of gust wavelength and high-lift propulsors on (a) shear force, (b) torsion and c) bending moment of the wing root for $V = 100$ m/s and $w_{ref} = 17.07$ m/s

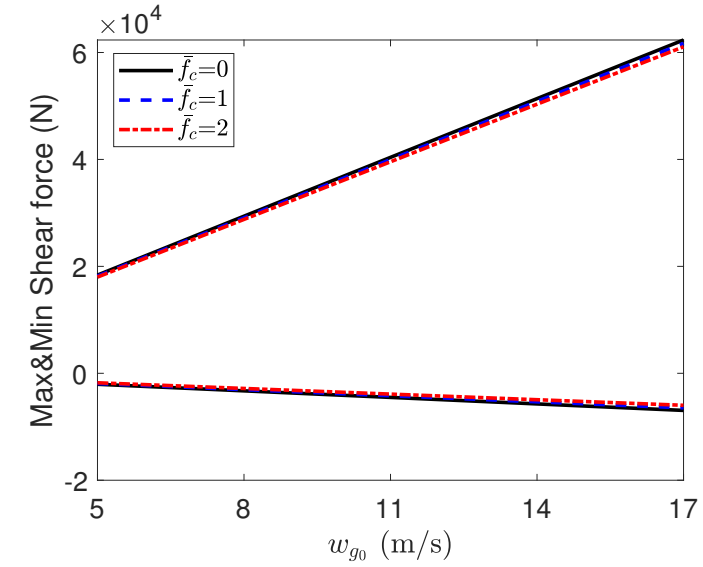

(a)

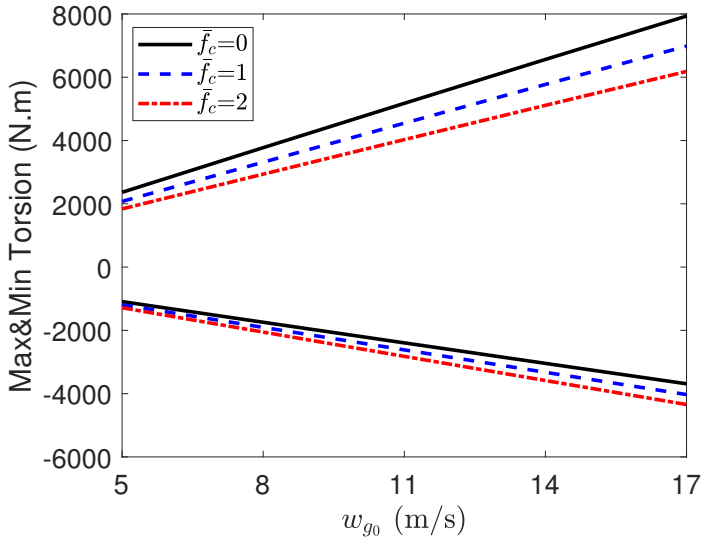

(b)

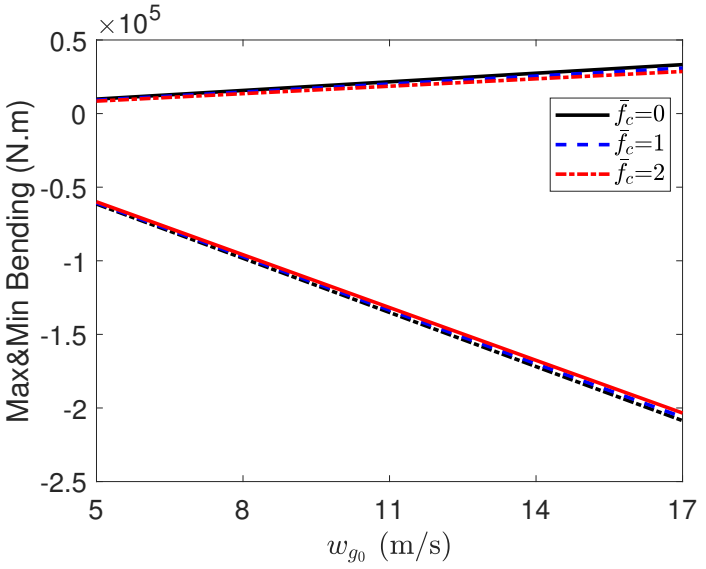

(c)

Figure 8: The effect of gust velocity and tip propulsor on (a) shear force, (b) torsion and c) bending moment of the wing root for $V = 100$ m/s and $l_g = 20$ m

two components in the chordwise and thicknesswise directions. That's why the gust loads are affected by thrust vectroing. As the maximum pitch angle increases, the gust loads are affected more. The results show that it is possible to reduce the maximum shear force and bending moment by up to 14% and 26%, respectively, while the torsional moment increases. This clearly highlights the potential influence of thrust vectoring on gust load reduction, even that here vectoring made the torsional load worse, but this will be discussed further in more details later.

The effect of thrust vectoring frequency on the maximum loads is shown in Figure 10. As it is expected, the best thrust vectoring which results in higher load reduction happens when the vectoring follows the same frequency of the gust. Therefore, from here on, this frequency is assumed for all case studies. Furthermore, still the torsional load doesn't decrease due to thrust vectoring. This is because that its assumed that the action point of the propulsor is exactly on the wing elastic axis, hence the thrust vectoring doesn't influence the torsional loads. However, if an offset in the chordwise direction from the wing elastic axis is considered, the thrust vectoring can become effective in reducing the torsional load as shown later.

Figure 11 shows the effect of gust wavelength and propulsor's thrust level on maximum gust loads. In this case, the thrust vectoring amplitude and gust velocity are assumed to be $\theta = -60^o$, and $w_{g_0} = 17$ m/s, receptively, while the vectoring frequency is assumed to be half of the gust frequency (e.g. $\omega_v = \frac{V}{2l_g}$). The results indicates that as the level of thrust vectoring increases, the maximum shear and bending loads decrease by almost the same factor as thrust change. However, the torsional load still is not so sensitive to the thrust vectoring.

Figure 12 shows how the chordwise offset between the wing elastic axis and the thrust vectoring action point can influence the QIs. It is clear that as the action point shifts toward leading edge, the effectiveness of the thrust vectoring increases. Now, in this case, the wing root torsional moment also decreases. Therefore, to make the thrust vectoring more effective, the propulsors should be mounted as far as possible from the elastic axis and toward the wing leading edge. It is noted that moving the propulsors toward leading edge could also be beneficial for aerodynamic performance as described in [6].

Finally, the effect of thrust vectoring on gust load alleviation of the aircraft for multiple flight points within the flight envelope of the aircraft is investigated. Figure 13 shows 20 flights points within the flight envelop of the aircraft. It is noted that this flight envelope is not the actual flight envelop of the NASA X-57, but is close to it [28]. Figure 14 shows the convex hull of the maximum gust loads at the wing root with and without thrust vectoring. Here, 20 flight points are combined with 10 gust wavelength ranging from 10 m to 100m (equally spaced), which gives 200 gust load cases. I this case, the thrust vectoring angle is set as $\theta = 60^o$ and it is assumed that the propulsor is located 40% of the chord from the elastic axis toward the leading edge. It is clear that thrust vectoring successfully reduced the critical load combinations. Not only this, but also it reduced the region inside the convex hull. This clearly shows that using a thrust vectoring has the potential to be effective in gust load alleviation of next generation electric aircraft. It is noted that here, the aerodynamic and inertia influences of the propellers are ignored, while they can affect the results. This will be investigated in future studies.

5 CONCLUSION

A new concept for gust load alleviation of aircraft wings with distributed electric propulsors was proposed. The concept is based on pitching the propulsors thrust vector sinusoidally. The aeroelastic model of the wing was developed by combining an exact beam formulation with an unsteady aerodynamic theory. A "1-cos" gust profile with various gust reference velocity and wavelength was considered. The results showed that the tip propulsor affects the gust loads

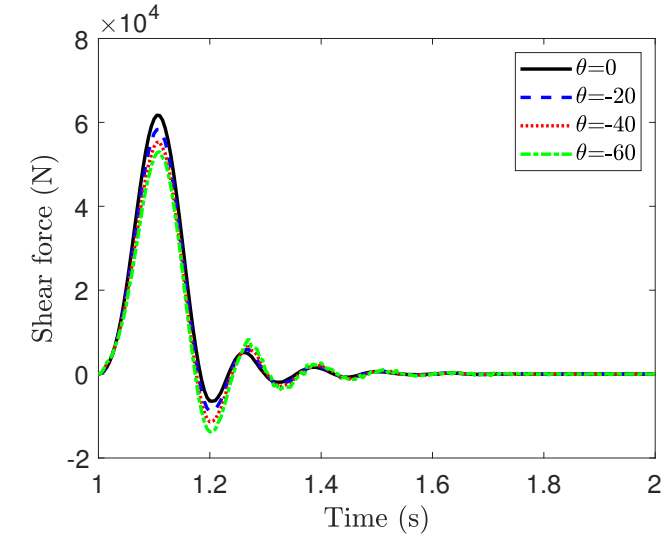

(a)

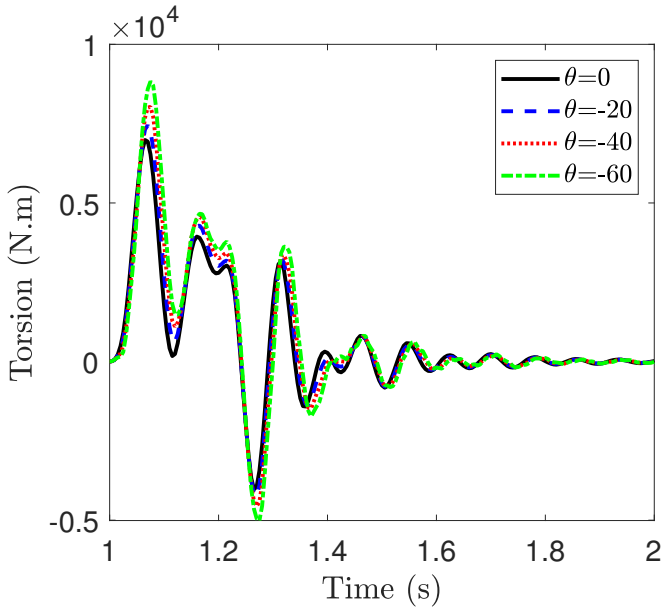

(b)

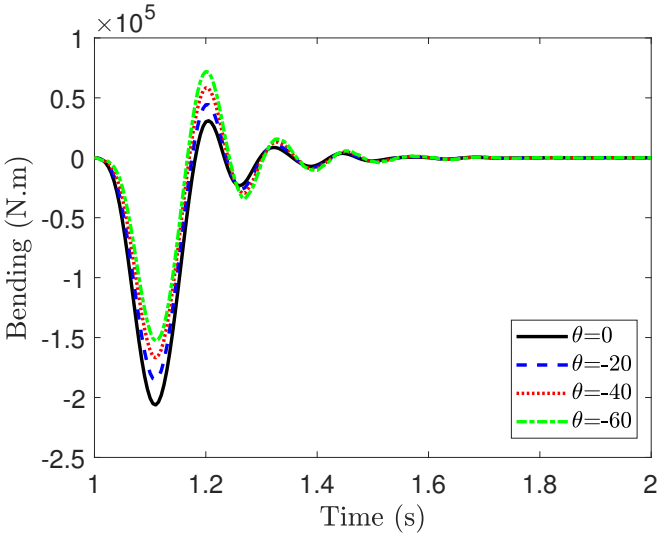

(c)

Figure 9: The effect of thrust vectoring pitch angle on the (a) shear force, (b) torsion and c) bending moment of the wing root for $V = 100$ m/s, $l_g = 20$ m, $w_{g_0} = 17$ m/s, and $\omega_v = 2$ Hz

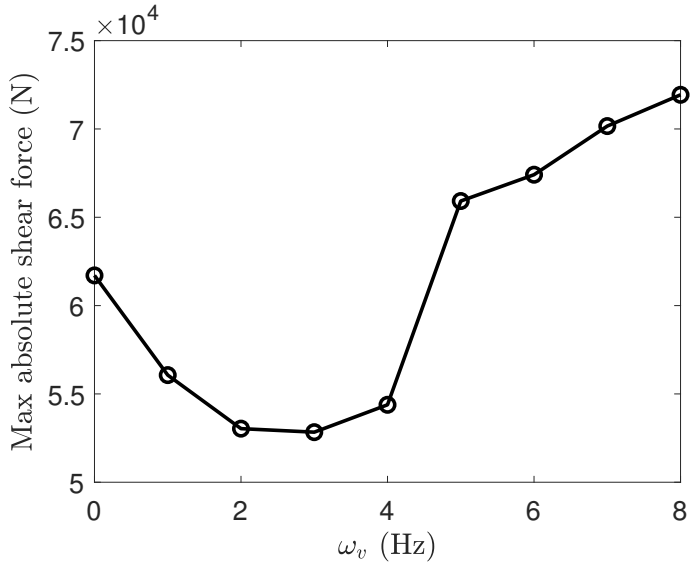

(a)

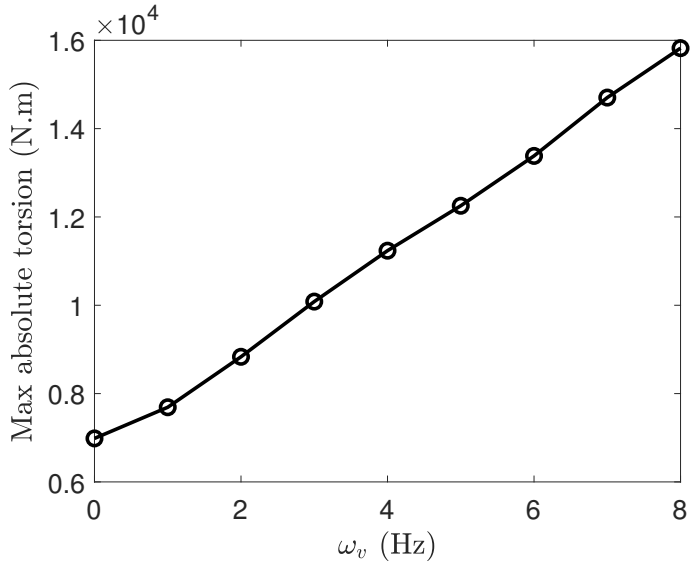

(b)

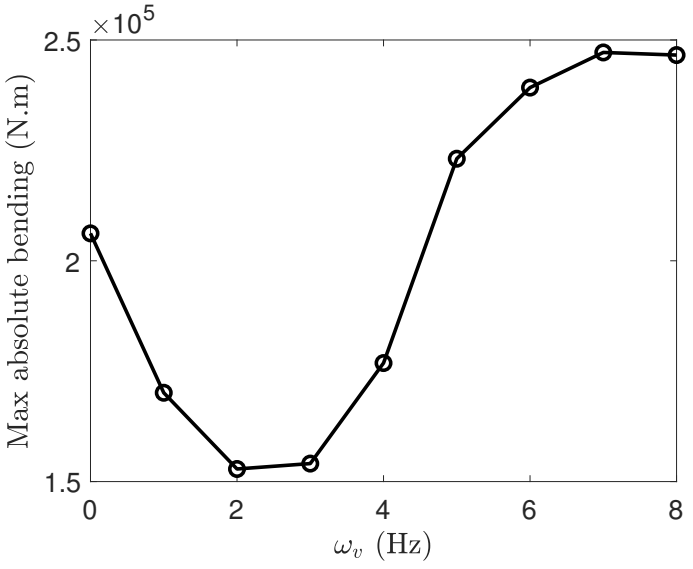

(c)

Figure 10: The effect of thrust vectoring frequency on the (a) shear force, (b) torsion and c) bending moment of the wing root for $V = 100$ m/s, $l_g = 20$ m, $w_{g_0} = 17$ m/s, and $\theta = -60$ Hz

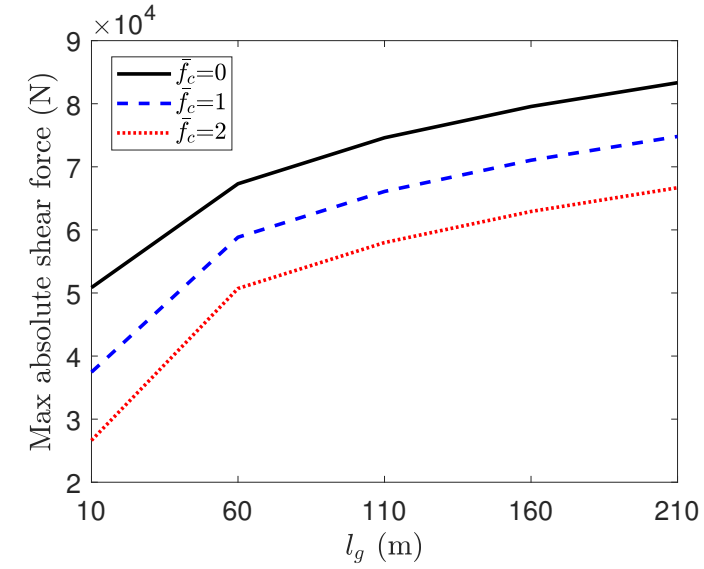

(a)

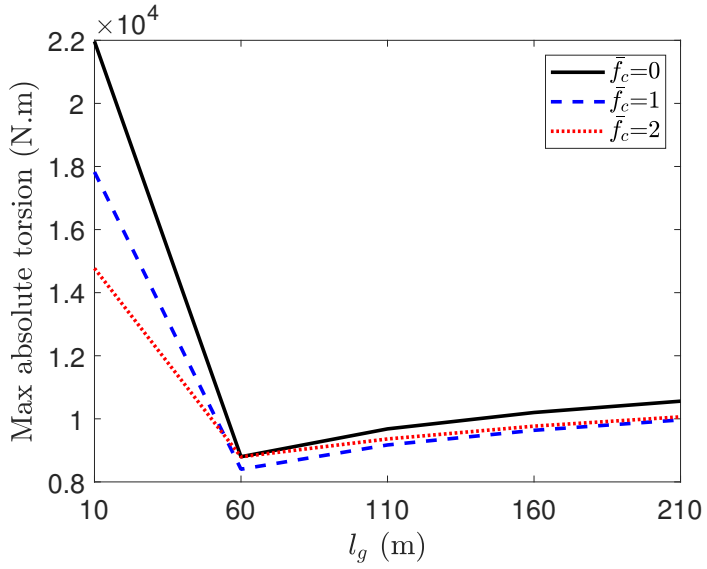

(b)

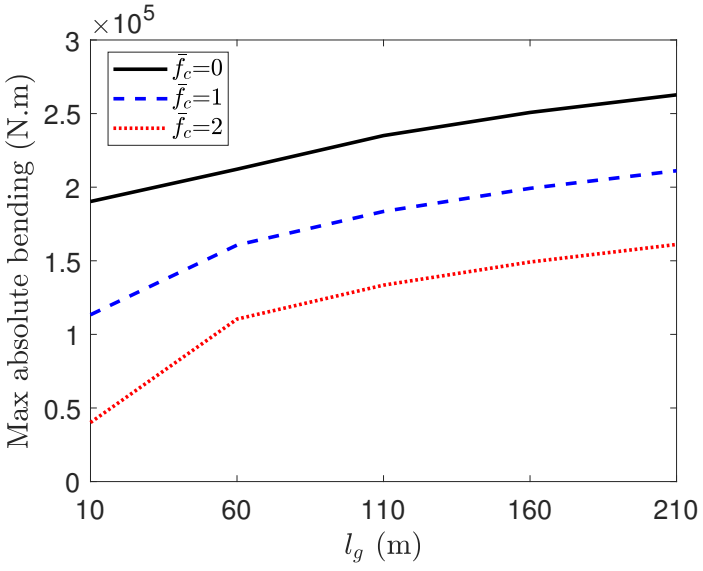

(c)

Figure 11: The effect of gust wavelength and thrust vectoring magnitude on the maximum absolute values of (a) shear force, (b) torsion and c) bending moment of the wing root for $V = 100$ m/s, $w_{g_0} = 17$ m/s, and $\theta = -60$ Hz

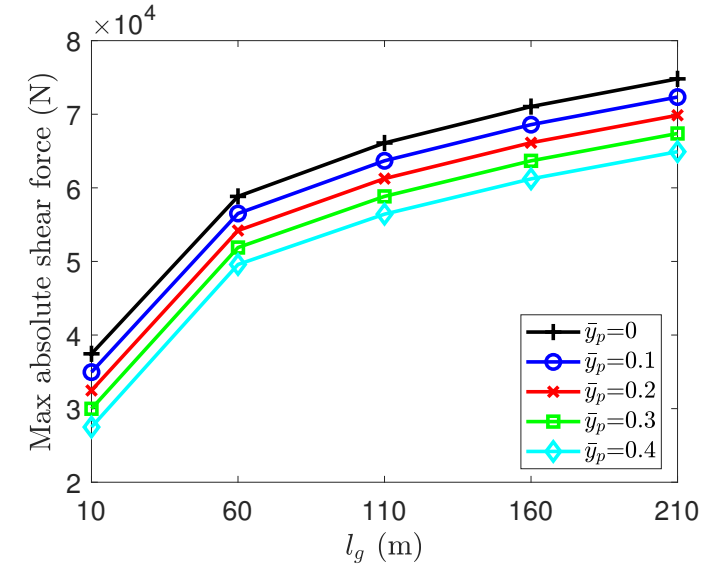

(a)

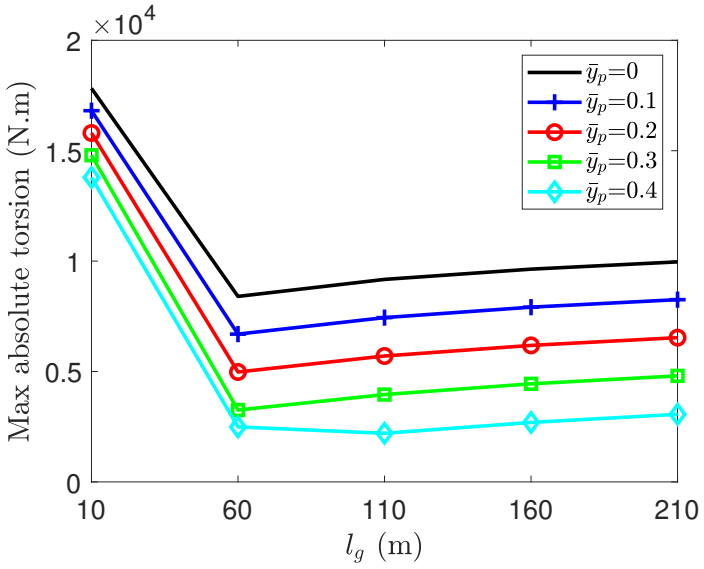

(b)

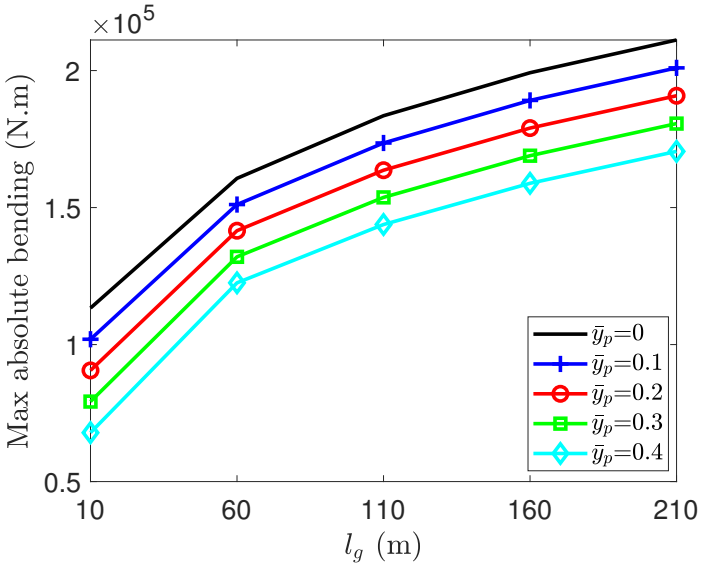

(c)

Figure 12: The effect of propulsor's chordwise offset and gust wavelength on the maximum absolute values of (a) shear force, (b) torsion and c) bending moment of the wing root for $V = 100$ m/s, $w_{g_0} = 17$ m/s, and $\theta = -60$ Hz

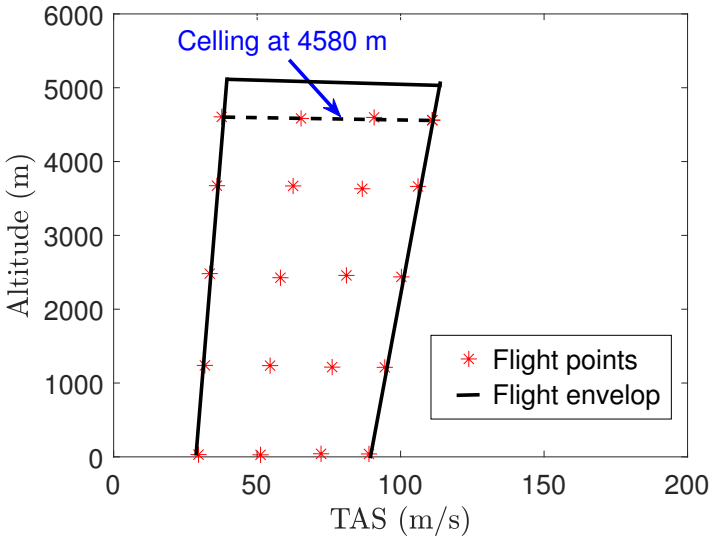

Figure 13: Flight points selected across the flight envelope

more than the high-lift motors. Also, it was found that by pitching the thrust vector with a frequency similar to the gust frequency leads to the best possible gust load alleviation. The bending moment and shear force were reduced significantly by pitching the thrust vector. the amount of reduction is related to the pitch angle. To reduce the torsional load, it is required to move the propulsor toward the leading edge of the wing. Also, the results showed that by increasing the thrust level, the load alleviation capability increases almost by the same factor as increasing the thrust level. Finally, the convex hull of a wing which resembles the NASA-X57 was determined with and without thrust vectoring, and it was obtained that by vectoring the thrust it is possible to reduce and shrink the convex hull for all combinations of quantities of interest. It is noted that in future studies the effects of propellers' aerodynamics and mass will be included, while ignored in this study, to fully analyse the capability of the proposed concept.

6 ACKNOWLEDGMENT

The first author gratefully acknowledge the support of the Royal Society through the research grant, RG\R1\241330, on "Gust loads of flexible wings with electric propulsors",.

COPYRIGHT STATEMENT

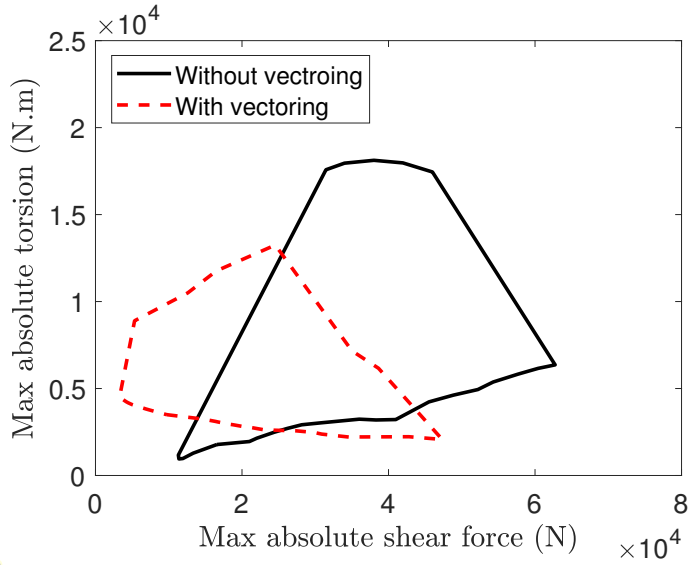

(a)

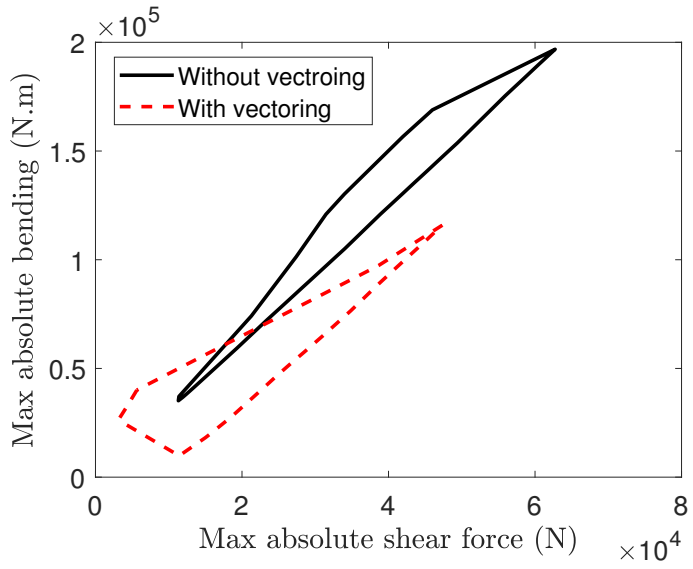

(b)

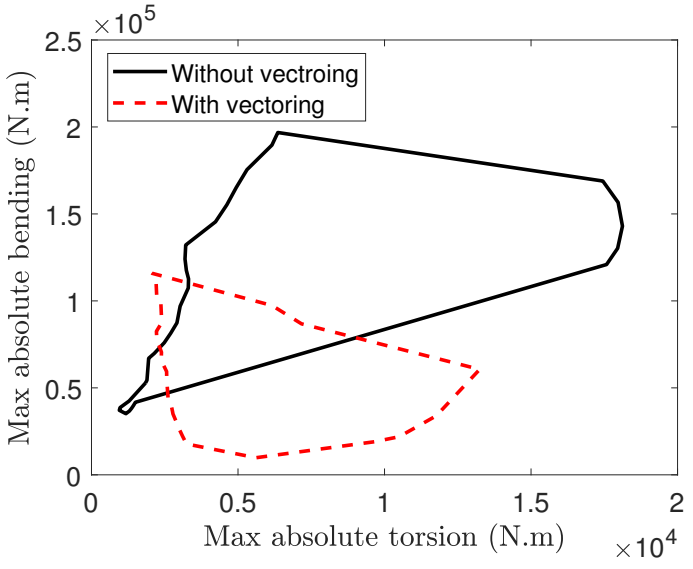

(c)

Figure 14: The effect of thrust vectoring on wing root a) shear force-torsional moment , b) shear force-bending moment, and c) torsional moment-bending moment for $w_{g_0} = 17m/s$, $\theta = -60$ m/s and $\bar{y}_p = 0.4$

7 REFERENCES

[1] Litherland, B. L., Borer, N. K., and Zawodny, N. S. (2021). X-57 maxwell high-lift propeller testing and model development. In *AIAA AVIATION 2021 FORUM*.

[2] Leifsson, L., Ko, A., Mason, W., et al. (2013). Multidisciplinary design optimization of blended-wing-body transport aircraft with distributed propulsion. *Aerospace Science and Technology*, 25(1), 16–28. ISSN 1270-9638. doi:https://doi.org/10.1016/j.ast.2011.12.004.

[3] Stoll, A. M., Bevirt, J., Moore, M. D., et al. (2014). Drag reduction through distributed electric propulsion. In *14th AIAA Aviation Technology, Integration, and Operations Conference*. Atlanta, GA.

[4] (2011). Challenges of future aircraft propulsion: A review of distributed propulsion technology and its potential application for the all electric commercial aircraft. *Progress in Aerospace Sciences*, 47(5), 369–391.

[5] Amoozgar, M., Hall, M., Dimitriadis, G., et al. (2024). The effect of thrust vectoring on aeroelastic stability of electric aircraft. In *AIAA SCITECH 2024 Forum*. Orlando, Florida.

[6] Patterson, M. D. and German, B. (2014). Wing aerodynamic analysis incorporating one-way interaction with distributed propellers. In *14th AIAA Aviation Technology, Integration, and Operations Conference*. Atlanta, GA.

[7] Ma, Y., Zhang, W., Zhang, Y., et al. (2020). Sizing method and sensitivity analysis for distributed electric propulsion aircraft. *Journal of Aircraft*, 57(4), 730–741. doi:10.2514/1.C035581.

[8] Erhard, R. M., Clarke, M. A., and Alonso, J. J. (2021). A low-cost aero-propulsive analysis of distributed electric propulsion aircraft. In *AIAA Scitech 2021 Forum*.

[9] Simmons, B. M. and Murphy, P. C. (2021). Wind tunnel-based aerodynamic model identification for a tilt-wing, distributed electric propulsion aircraft. In *AIAA Scitech 2021 Forum*.

[10] (2022). Design principles and digital control of advanced distributed propulsion systems. *Energy*, 241, 122788. ISSN 0360-5442.

[11] Fazelzadeh, S., Mazidi, A., and Kalantari, H. (2009). Bending-torsional flutter of wings with an attached mass subjected to a follower force. *Journal of Sound and Vibration*, 323(1), 148–162. ISSN 0022-460X.

[12] Amoozgar, M., Irani, S., and Vio, G. (2013). Aeroelastic instability of a composite wing with a powered-engine. *Journal of Fluids and Structures*, 36, 70–82. ISSN 0889-9746.

[13] Ghasemikaram, A. H., Mazidi, A., Fazelzadeh, S. A., et al. (2023). Engine placement effects on the flutter of a medium-range box-wing aircraft. *Journal of Aerospace Engineering*, 36(4), 04023024. doi:10.1061/JAEEEZ.ASENG-4753.

[14] Hodges, D. H., Patil, M. J., and Chae, S. (2002). Effect of thrust on bending-torsion flutter of wings. *Journal of Aircraft*, 39(2), 371–376.

[15] Amoozgar, M., Irani, S., and Vio, G. (2013). Aeroelastic instability of a composite wing with a powered-engine. *Journal of Fluids and Structures*, 36, 70–82. ISSN 0889-9746. doi:https://doi.org/10.1016/j.jfluidstructs.2012.10.007.

[16] Otsuka, K., del Carre, A., and Palacios, R. (2022). Nonlinear aeroelastic analysis of high-aspect-ratio wings with a low-order propeller model. *Journal of Aircraft*, 59(2), 293–306.

[17] Szczyglowski, C. P., Neild, S. A., Titurus, B., et al. (2019). Passive gust loads alleviation in a truss-braced wing using an inerter-based device. *Journal of Aircraft*, 56(6), 2260–2271.

[18] Khodaparast, H., Georgiou, G., Cooper, J., et al. (2012). Rapid prediction of worst case gust loads. *Journal of Aeroelasticity and Structural Dynamics*, 2(3), 33–54. ISSN 1974-5117.

[19] Amoozgar, M., Castrichini, A., Garvey, S., et al. (2024). The effect of a nonlinear energy sink on the gust response of a wing. *Aerospace Science and Technology*, 145, 108904. ISSN 1270-9638. doi:https://doi.org/10.1016/j.ast.2024.108904.

[20] Castrichini, A., Hodigere Siddaramaiah, V., Calderon, D. E., et al. (2016). Nonlinear folding wing tips for gust loads alleviation. *Journal of Aircraft*, 53(5), 1391–1399.

[21] Healy, F., Cheung, R. C., Rezgui, D., et al. (2022). On the nonlinear geometric behaviour of flared folding wingtips. In *AIAA SCITECH 2022 Forum*. doi:10.2514/6.2022-0656.

[22] Khalil, A. and Fezans, N. (2021). Gust load alleviation for flexible aircraft using discrete-time. *The Aeronautical Journal*, 125(1284), 341–364.

[23] Hodges, D. H. (2003). Geometrically exact, intrinsic theory for dynamics of curved and twisted anisotropic beams. *AIAA Journal*, 41(6), 1131–1137.

[24] Peters, D. A., Karunamoorthy, S., and Cao, W.-M. (1995). Finite state induced flow models. i - two-dimensional thin airfoil. *Journal of Aircraft*, 32(2), 313–322.

[25] Amoozgar, M., Ajaj, R., and Cooper, J. (2022). The effect of elastic couplings and material uncertainties on the flutter of composite high aspect ratio wings. *Journal of Fluids and Structures*, 108, 103439. ISSN 0889-9746.

[26] Amoozgar, M., Fazelzadeh, S., Haddad Khodaparast, H., et al. (2020). Aeroelastic stability analysis of aircraft wings with initial curvature. *Aerospace Science and Technology*, 107, 106241. ISSN 1270-9638.

[27] Amoozgar, M., Friswell, M. I., Fazelzadeh, S. A., et al. (2021). Aeroelastic stability analysis of electric aircraft wings with distributed electric propulsors. *Aerospace*, 8(4).

[28] Borer, N. K., Geuther, S. C., Litherland, B. L., et al. (2018). Design and performance of a hybrid-electric fuel cell flight demonstration concept. In *2018 Aviation Technology, Integration, and Operations Conference*. Atlanta, Georgia.